Optimisation and hydrodynamic analysis of a bottom-hinged surge wave energy converter

Guilherme Leão Albuquerque Estrela Geraldes

Centre for Marine Technology and Ocean Engineering (CENTEC), Instituto Superior Técnico

University of Lisbon, Portugal

December 2017

Abstract

The objective of this dissertation is to study the energy converter that, based on its oscillatory movements, is able to extract the energy from the almost horizontal motion of the water particles in shallow waters. This converter, which is known as oscillating surge wave energy converter, is already being deployed in some European coastlines. To be able to examine the effects of varying the converter main dimensions in the amount of generated power, a semi-analytical analysis of the potential flow around the device was realised, considering the diffraction and radiation potentials, by using the Green's integral Theorem. To validate the results, obtained with the semi-analytical method, experimental analyses were realised aiming to verify if the theoretical results follow the same tendencies as the experimental trials. An analysis of the Portuguese waves' characteristics was done so that the device's responses could be evaluated to understand how their dimensions comply with incident waves.

Keywords: Wave energy converter, Renewable Energy, Wave energy, *OSWEC*, Green's integral Theorem

1. Introduction

The present work aimed to analyse the hydrodynamics of an Oscillating Surge Wave Energy Converter, *OSWEC*, and to experimentally validate the equations that describe these devices. The equations were developed mainly for the analysis of devices whose upper surface extends above the water's free surface, as studied by Henry [13], van't Hoff [28], Renzi and Dias [21]. However, by changing the integral limits of these equations, it is possible to used them to evaluate submerged devices. Yet, until today, no validation has been realised to these equations when evaluating submerged devices. So, after the analysis of the resultant values of these equations, experimental tests were realised enabling the chance of comparing them with theoretical results for both the surface piercing and the submerged devices.

To obtain the theoretical equations that describe these devices, it was necessary to use a method developed by Haskind, in the beginning of the *60s*, with the goal of determining the forces that are applied on a ship by an incident wave system. However, besides the need of knowing the incident waves' hydrodynamic pressure, it is also necessary to know the effects caused by the presence of the body on this pressure field. The equations derived by Haskind for the exciting forces and the moments on a fixed body which do not require the knowledge of the diffraction effects caused by the body's presence. These equations are based on a demonstration made by Haskind which confirmed that the velocity potential at a large distance from the body is sufficient to determine the exciting forces for a given incident wave system, as Newman stated in [17]. For many problems, this solution can expedite the calculation of the exciting forces and the moments applied on a body because it is too complex to determine the near-field forced-oscillation potential or the diffraction potential [17]. So, the semi-analytical equations are based on a linear relation obtained by Haskind between the exciting forces exerted on a fixed body by the incident waves and the amplitude of the far-field radiated waves generated by the forced motions of the body in otherwise calm water.

These semi-analytical equations were already used by Renzi and Dias [20, 21] to evaluate surface piercing *OSWECs*. So, the equations were implemented in a *MatLab* algorithm enabling the opportunity of varying the main device's dimensions and also the height of the device in relation with the local water depth. Among other assumptions, it was necessary to assumed potential flow theory, with regular and monochromatic propagating waves.

If these semi-analytical equations are validated experimentally, it will be possible to reduce the costs associated with the optimisation of the device's dimensions towards a certain wave climate using experimental tests [9]. These still need to be realised however, it would only be necessary to evaluate the dimensions that had been optimised theoretically.

2. Background

Since the disclosure of the first electric generator, by Faraday in the *1830s*, that the rotor is mainly powered by the combustion of non-renewable fuels. While the dangers resulting from the combustion of these fuels were unknown and their prices were relatively cheap, there was no need to change the fuels that were being used. Yet, in the 70s, when a war between the Arabs and the Israelis erupted, it resulted in an oil-embargo which reduced the monthly oil production to *5%* of its usual value. This led to an unreasonable increase in the oil prices', shifting the attention towards cheaper alternatives which could be the renewable sources of energy, for example, solar, eolic, hydric, thermal or wave energy.

2.1. Wave Energy

The wave energy originates from the dynamisation realised by the solar energy on the eolic energy. So, the advantage of using the waves' energy is because it is a concentrated form of wind energy, as stated by [5, 22]. Yet, it is necessary to investigate the availability of this resource. Gunn and Stock-Williams [12] estimated the total amount of available wave energy as being *2.11 TW ± 0.05 TW*. This result is comparable to older estimates, like the ones by Kinsman [15] and Inman and Brush [14] where they stated that the global wave power was *1.87 TW* and *2.5 TW*, respectively. At the time, these estimates enabled the determination of the upper and lower wave energy values that would reach the shore-

lines. However, nowadays there are programs that enable a more reliable quantification of the wave potential resource. Gunn and Stock-Williams [12] used one of the state-of-the-art programs, the *WaveWatch III, WWIII*, for wave generation and swell propagation, enabling the determination of the amount of energy flux that crosses a line distanced *30* nautical miles from shore. These results would then be used as boundary conditions for the model that simulates waves in the nearshore region called *Simulating Waves Nearshore, SWAN*. This combination between *WW3*, for the analysis of wave generation and swell propagation, and then *SWAN*, for nearshore region analysis, is commonly realised for the evaluation of the nearshore region waves' potential energy, like Silva et al. [25] did for the analysis of the waves' energy in the Iberian Peninsula. However, it is also possible to use other combinations such as using the *Wave Modelling*, *WAM*, for the boundary conditions of the *SWAN* model, as was done by Rusu and Guedes Soares [23] when estimating the spatial distribution of wave energy in the Portuguese nearshore.

The Portuguese southern and western coastlines are bathed by the Atlantic Ocean and, as was concluded by Gunn and Stock-Williams [12], the western shores are predominantly bathed by more energetic waves because the primary waves' direction is from west to east. From the analysis realised by Silva et al. [25], it is possible to obtain the prediction of mean wave power for certain Portuguese regions and for Figueira da Foz during the winter it reached *47 kW/m* and in the summer *5.5 kW/m*.

2.2. Wave Energy Converters

Wave energy conversion technology started to be developed at more than *200* years ago and the first known patent for a wave energy converter is dated to *1799* [3]. At the time, due to the fact that the generator hadn't yet been revealed, the aim, for the use of this device, was to power tilt hammers, saws, mills, or other tools that required mechanical power. Since then, and during the period between *1856* and *1973*, it is estimated that the United Kingdom granted *340* patents on devices that claimed to be able to utilise wave energy as their source of power, as was stated by Leishman and Scobie [16].

Due to the oil embargo that occurred in *1973*, several investigators started to focus on renewable energies and one of which was Stephen Salter, the creator of the Salter's duck [24]. During his investigation he managed to conclude, by analysing the governing equations of the maximum efficiency, E_{max}, that he needed to design the device's shape so that its oscillations could not transmit waves past the device, as can be deduced by:

$$E_{max} = \frac{|A_U|^2}{|A_U|^2 + |A_D|^2}\,, \tag{1}$$

where A_U are the wave amplitudes upstream from the device and A_D are the wave amplitudes downstream from the device, when the waves are flowing from upstream to downstream. If the amplitude of the waves downstream from the device are comparatively smaller than the upstream ones, then it is possible to conclude that most of the incident wave energy was absorbed by the device.

During Stephen Salter's experiences, he started with a device that had *15%* of efficiency which simply bobbed up and down. By adding a hinge below the water surface, he was able to increase the efficiency up to *60%* however, the device's motion was generating and reflecting waves. So, he started modifying the device's shape to decrease the amplitude of the reflected waves, reaching an efficiency of *90%* which was the *Salter's duck* shape.

The optimisation process, for the main device's dimensions, could be realised ideally solely using the semi-analytical equation. However, before reaching that stage, it is necessary to determine the characteristics that define the site where the device will be deployed.

The initial phase for the design process of a *WEC* starts by selecting the depth in which the device will be placed. While some of them are designed for the offshore region, there are others that need to be placed in shallow waters. While some oscillate around an axis others can move freely. Due to their specific characteristics there are several methods that enable the categorisation of wave energy converters. They can be categorised either by the location where they will be placed, or by their size and directional characteristics, or, even, by their working principle.

2.2.1. Placement of a Wave Energy Converter

This method of categorising *WECs* is based in the division of the ocean in three distinct areas, using the water depth as a variable. The resultant division, that ranges between the deep waters to the onshore depth, is: offshore, nearshore and onshore devices.

The placement of devices in the offshore region, in depths larger than *40 m*, is with the intention of extracting more power from the more energetic seas. Due to their location, the reliability and survivability of these devices is a big problem because they are more prone of interacting with extreme seas which would impose higher loads on the structure. As they are more distant from the shore, it is expected that their implementation and maintenance costs are higher when compared with the devices that are closer to shore.

The advantage of placing devices in the nearshore region, where the depths range between *10* up to *25 m*, is due to their smaller implementation and maintenance costs, relatively to the devices that are placed on the offshore region. This reduction of costs is a consequence of placing the devices in smaller depths which, usually, only occur in sites nearer the shore. However, due to this proximity to the sea floor, the energy of the waves suffer more predominantly from the shoaling effects, as stated by Whittaker and Folley [30]. This can be compensated by the fact that, in this region, the devices are less prone to extreme wave events and the waves' dimensions suffer less variability, which can be attributed to the shoaling effects and to the depth limited wave height. Due to the smaller depths, the device can rest on the seabed avoiding the need for moorings which would be necessary for deep water devices.

The last possibility, for the placement of a wave energy converter, is onshore. These devices can be placed above the sea, integrated in a breakwater, in a dam, or fixed to a cliff. The main advantage of these converters is their easier maintenance and installation because, in most cases, their location is easily accessible. Due to the proximity to shore the waves are even more affected by the bottom friction which reduces the incident wave energy. The sites where these devices can be installed need to be thoroughly checked because the devices will probably reshape the shore and the bottom surface.

The device that is going to be analysed is usually placed in the nearshore region with water depths that range between *10* up to *25 m*. The loss of energy, due to the passage from

deep waters to shallower waters, varies and depends of a couple parameters which are: the wave period, the wave height and, also, the total depth variation. Whittaker and Folley [30] analysed the variation in wave energy due to the passage from depths of *50 m* to depths of *10 m* for four different bathymetry profiles: *1:50*, *1:100*, *1:200* and *1:500*. From the results, they verified that the energy loss was higher for the cases that had a smaller gradient. Which means that the waves that covered sea slopes with an inclination of *1:500* would reach the *10 m* depth with less energy than when they covered the slope with an inclination of *1:50*, due to the shorter longitudinal distance that they had to travel. For waves advancing towards the shore, coming from deep waters with a bottom gradient of *1:100*, the loss of energy can be analysed in *Figure 1*.

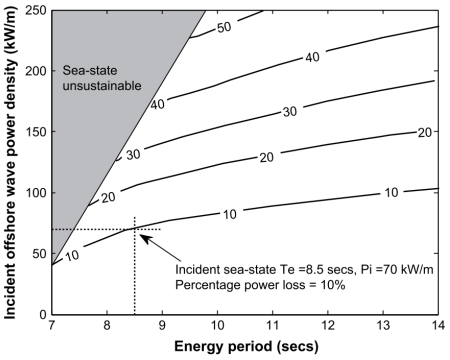

Figure 1: Wave energy loss with a bottom slope of *1:100* from the deep to shallow waters (Whittaker and Folley [30])

For waves with power levels between *50 kW/m* and *100 kW/m* it can be said that the energy losses will vary between *10 %* and *20 %* which seem to settle the doubts about the losses due to depth transition.

2.2.2. Orientation of a Wave Energy Converter

The device's dimensions and their orientation, with respect to the incoming waves, is another parameter that can be used to categorise the several types of *WECs*. With this categorisation method it is possible to aggregate devices that can be placed in different regions even if they use the same methods for extracting waves' energy. The devices can either be: an attenuator, a terminator or a point absorber.

The attenuator type of device has a long length, of the order of the wave length, and a width which is, comparatively, much shorter. The format of this device is identical to a snake formed by *4* or *5* elements which are interconnected between each other with a hydraulic system that will damp the device's motion and extract the energy from their relative oscillations. When placing this device, and to extract the most energy from the incident waves, it must be oriented along the direction of waves' propagation. The goal of this device, which is usually formed by a set of connected bodies, is to attenuate the motion of the waves. The most known device of this category is the *Pelamis*, a prototype converter with *750 kW* that was placed in the Portuguese shore and it powered partially a Portuguese city called Póvoa de Varzim.

The dimensions of the terminator type of device are similar to the ones of the attenuator however, instead of being oriented along the direction of waves' propagation it should have its biggest side oriented parallel to the crest of the waves. Its main dimension, which is its width, can reach values of *26 m*, like the renewed *Oyster Aquamarine version 2* [GTE]. The height of this device, depending if it is a surface piercing or a completely underwater device, can reach values up to *11 m*. This type of device has already been deployed, in the beginning of *2010*, for testing purposes and, with the obtained results, improvements were made to the device originating in a renewed second version, like stated by Cameron et al. [4]. There are several examples of devices that fit into this category, such as the *Salter's duck*, the *WaveRoller [AWE]* or the *Oyster Aquamarine*.

Finally, there is the point absorber type which, when compared with the previous types, has a smaller length and width but, probably, will have a larger height, when it is placed in deep waters. This type of device, instead of being oriented in respect with the direction of waves' propagation, it can be freely oriented because it is able to extract energy from all directions. The energy generation is done either by the bobbing of the device, in the upward and downward direction, or by using the variation of the height of the waves' free-surface. There are a lot of devices that fit in this category because, usually, these devices are placed in deep waters where the available energy is higher.

The device that is going to be analysed is classified as a terminator due to its perpendicular orientation with the direction of propagation of the waves.

2.3. Oscillating Surge Wave Energy Converter

The equations that eased the possibility of analysing *OSWECs* began with the investigation realised by Haskind which was then transcribed by Newman [17]. His method enabled the possibility of obtaining the values of the excitation forces applied on bodies by the incident waves. Haskind was interested in calculating the excitation forces without the laborious work of calculating the diffraction effects, or the forced-oscillation potential, which can be arduous to calculate, as stated in *1962* by Newman [17]. So, the goal was to determine an expression that allowed the calculation of the excitation forces for a given incident-wave system by simply using the asymptotic characteristics of the velocity potential at a large distance from the body.

During this period of time, between *1970 and 1990*, David Evans was interested in developing a theory that could predict the amount of absorbed power from an incident sinusoidal wave train by means of a damped, oscillating, partly or completely submerged body. Evans published a couple of scientific documents where he exposed theories for the calculation of the wave-power absorption for a single oscillating body and for two oscillating bodies, [10] and [26], respectively. He stated that the efficiency of this kind of system could be calculated by a proportion between the extracted power and the incident wave power, which would clearly depend on the details of the coupling between the device and the fluid. He also stated that the calculation of the maximum efficiency could be obtained without knowing the details of the coupling, either by using *Eq. 1* or by using a similar formula published by Newman [18], where he related the upstream complex coefficient that represents the wave amplitude, A_U, the downstream complex coefficient that represents the wave amplitude, A_D, with the coefficients of reflection and transmission of waves, R_w and T_w, respectively. The obtained relation is given by:

$$A_U + \bar{A}_U \cdot R_w + \bar{A}_D \cdot T_w = 0, \tag{2}$$

By considering the linear theory, solely the cases that cause small amplitude responses can be evaluated correctly. For

higher wave amplitudes, or higher response amplitudes, non-linear effects will start to have more importance. However, for an initial analysis considering solely the linear terms the resultant values represent an upper bound of the efficiency because it is generally accepted that the non-linear effects will tend to reduce it, as stated Evans [11].

3. Implementation

The method that is going to be explained enables the analysis of an oscillating surge wave energy converter, *OSWEC*, and is based on a semi-analytical model that assumes the fluid to be inviscid and incompressible while the flow must be irrotational and the perturbation time-harmonic. For a flow with such characteristics it is possible to define a velocity potential given by $\Phi'(x', y', z', t')$ that satisfies the Laplace equation:

$$\nabla^2 \Phi'(x', y', z', t') = 0\,, \tag{3}$$

the usage of primes is to represent the physical dimensions of the variables. The main dimensions that will be dealt with, when using this method, are:

Table 1: Definition of the main parameters for the semi-analytical model

Dimension	Variable	Units
Flap width	w'_f	[m]
Flap height	h'_f	[m]
Flap thickness	t'_f	[m]
Height of the hinge	c'	[m]
Local water depth	h'	[m]
Wave amplitude	A'_w	[m]
Wave period	T'	[s]

The semi-analytical model is based on the first-order analysis of a higher-order phenomena. By considering the linearised theory, the resultant values will represent a basis for further development. This theory imposes that the amplitude of the response angle and the amplitude of the incident waves must be small, when directly compared with the main dimension of what is being studied. In this case the ratio between the wave amplitude and the flap width must be small, which can be represented as $A'_w/\mathrm{w}'_f \ll 1$.

By linearising the boundary conditions, it is possible to obtain a combined boundary condition at the free surface that must be met by the velocity potential. The resultant equation is:

$$\frac{\partial^2 \Phi'}{\partial t'^2} + g\,\frac{\partial \Phi'}{\partial z'} = 0\,, \tag{4}$$

where g is the acceleration due to the gravity and this equation must be validated at the free surface, specifically at $z = 0$, with the *z-coordinate* pointed upwards with its origin at the free surface.

With the boundary conditions defined at the free surface, it is also necessary to enforce that the velocity potential must comply with the impermeability of the bottom surface which means that the fluid cannot pass through this surface. So, the vertical component of the fluid velocity through the bottom surface must be zero which gives the relation:

$$v_z\big|_{z=-h} = 0 \;\Leftrightarrow\; \frac{\partial \Phi'}{\partial z'}\bigg|_{z=-h} = 0\,. \tag{5}$$

It is also necessary to impose that longitudinal component of the velocity potential must be equal to the flaps' oscillatory velocity, expressed by:

$$\frac{\partial \Phi'}{\partial x'} = -\frac{\partial \theta'}{\partial t'} \cdot (z' + h' - c') \cdot H(z' + h' - c')\,, \quad at \quad x' = 0\,, -\frac{w'_f}{2} < y' < \frac{w'_f}{2}\,, \tag{6}$$

The velocity potential of the fluid flow is a function that is dependent of both the location and the time. It can be defined by the sum of the velocity potentials that influence its propagation. This resultant velocity potential can be represented by:

$$\Phi(x, y, z, t) = \mathrm{Re}\left\{\left(\phi^I + \phi^D + \phi^R\right) \cdot e^{-i\omega t}\right\} = \mathrm{Re}\left\{\left(\phi^S + \phi^R\right) \cdot e^{-i\omega t}\right\}\,, \tag{7}$$

where ϕ^I is the incident wave potential, ϕ^D is the diffracted wave potential and ϕ^R is the radiated wave potential. The incident wave potential which is independent of the flaps' presence, can be determined by:

$$\phi^I = -\frac{iA_I}{\omega \cdot cosh(kh)} cosh\big(k(z+h)\big) \cdot e^{-ikx}\,, \tag{8}$$

where A_I is the dimensionless amplitude of the incident regular waves, h is the dimensionless local water depth, it has been assumed that the direction of the waves is from $x = +\infty$ to $x = -\infty$ and the dimensionless wave number, k, is obtained by solving the dispersion relation, given by:

$$\omega^2 = k \cdot tanh(kh)\,. \tag{9}$$

Besides the calculation of the wave number of the incident waves for a certain depth, h, and a given wave frequency, ω, it is necessary to consider the waves that are going to be radiated by the motion of the *WEC*. These waves can be radiated in a direction towards the origin of the incident waves or towards their original direction of propagation. However, there is a big difference in the propagation of these waves because they are characterised as being evanescent which, numerically, can be settled by using imaginary wave numbers, $k = i\kappa$. It is necessary to resort to these imaginary wave numbers because these evanescent waves need to decay exponentially instead of propagating towards infinity, with no variation. By replacing these imaginary terms in *Eq. 9* and by using the trigonometric relations, it is possible to achieve the following relation:

$$\omega^2 = -\kappa \cdot tan(\kappa h)\,, \tag{10}$$

This relation is needed to obtain the infinite amount of wave numbers of the evanescent waves which can be obtained by solving *Eq. 10*.

The flap's motion needs to be imposed as a boundary condition to the radiated velocity potential, resulting in:

$$\frac{\partial \phi^R}{\partial x} = V \cdot (z + h - c) \cdot H(z + h - c)\,,\;\; x = 0\,,\; -\frac{1}{2} < y < \frac{1}{2}\,, \tag{11}$$

where $V = i\omega\theta$. Having settled the boundary conditions that need to be imposed to the radiated velocity potential, it is still necessary to define the diffracted velocity potential. Experimentally, the scattered potential can be determined by fixing the flap at its vertical position with the propagating waves striking the device. Analytically the diffracted potential will be defined as being equal to the inverse of the incident wave potential, given by:

$$\phi^D = -\phi^I\,, \qquad x = 0\,, \quad -\frac{1}{2} < y < \frac{1}{2}\,. \tag{12}$$

The velocity potential, $\Phi(x, y, z)$, varies with three variables which are: x that is directed along the waves' direction of propagation, y that is directed perpendicularly to the

waves' direction of propagation and z that is directed perpendicularly in the upward direction in relation to the free surface. This velocity potential can suffer a separation of variables and the vertical coordinate can be defined by a single function, $Z(z)$. This function can be determined by applying the boundary conditions, that can be seen in *Eq. 4* and in *Eq. 5*, and it is also necessary to impose the Laplace equation, given by *Eq. 3*. A problem with such boundary conditions is known as being of the Stürm-Liouville type, resulting in:

$$Z_n(z) = \frac{\sqrt{2}\cdot cosh\big(k_n\cdot(z+h)\big)}{\sqrt{h+\omega^{-2}\cdot sinh^2(k_n\cdot h)}}\,,\quad atn = 0,1,2,...,N \tag{13}$$

When considering that the radiated waves are evanescent, it is necessary to use imaginary wave numbers, $k_n = i\kappa_n$. So, by replacing the imaginary wave numbers in *Eq. 13*, it takes the following format:

$$Z_n(z) = \frac{\sqrt{2}\cdot cos\big(\kappa_n\cdot(z+h)\big)}{\sqrt{h-\omega^{-2}\cdot sin^2(\kappa_n\cdot h)}}\,,\quad n = 1,2,...,N \tag{14}$$

The resultant separation of variables for the velocity potential, $\Phi(x,y,z)$, results in the following equation:

$$\phi^{(R,D)}(x,y,z) = \sum_{n=0}^{N}\varphi_n^{(R,D)}(x,y)\cdot Z_n(z)\,, \tag{15}$$

The first term, $n=0$, corresponds to the propagating wave and the subsequent terms, for $n>0$, are the evanescent modes generated by the radiated waves. Renzi and Dias [20] concluded that the calculation of the velocity potential converges quickly for values of $N\geq 4$ with virtually no error. So, by considering solely *4* evanescent wave numbers it is possible to obtain very small relative errors when calculating the velocity potential of both the radiated and the diffracted waves.

It is necessary to define the expression for the radiated velocity potential which is given by:

$$\begin{aligned}&\frac{\partial\sum_{n=0}^{N}\varphi_n^{(R)}(x,y)}{\partial x} = \\ &= \frac{\sqrt{2}V\cdot\Big[k_n h_f\cdot sh\big(k_n(h_f+c_f)\big) - ch\big(k_n(h_f+c_f)\big)\Big]}{k_n^2\cdot\sqrt{h+\omega^{-2}\cdot sh^2(k_n\,h)}} + \\ &+ \frac{\sqrt{2}V\cdot\Big[ch\big(k_n\,c_f\big)\Big]}{k_n^2\cdot\sqrt{h+\omega^{-2}\cdot sh^2(k_n\,h)}} = V\cdot f_n\,,\end{aligned} \tag{16}$$

Lacking, finally, the expression for the diffracted velocity potential, given by:

$$\frac{\partial\sum_{n=0}^{N}\varphi_n^{(D)}(x,y)}{\partial x} = A_I\cdot\frac{k_n\cdot\sqrt{h+w^{-2}\cdot sinh^2(k_n\,h)}}{\sqrt{2}\cdot\omega\cdot cosh(k_n\cdot h)}\,, \tag{17}$$

Knowing the equations that are necessary to use the semi-analytical method, it is required to define the hydrodynamic parameters for this type of device.

3.1. Hydrodynamic Parameters

Prior to the presentation of the hydrodynamic equations that characterise an *OSWEC*, it is necessary to settle that the analysed *WEC* was assumed to be immersed in a fluid with density ρ and that it will be influenced by the unsteady flow that will be created around the body. The flaps were assumed as being of rectangular parallelepiped shape so, the inertia of the device' flap can be calculated by the following formula:

$$I_f = \frac{1}{3}\cdot\rho_f\cdot t_f\cdot \mathrm{w}_f\cdot h_f^3\,, \tag{18}$$

where ρ_f is the volumetric density of the flap, t_f is the thickness of the flap, w_f is the width of the flap and h_f is the height of the flap, as was presented by Dhanak and Xiros [8].

The equation that enables the calculation of the hydrostatic restoring moment is present in Dhanak and Xiros [8] and it can be obtained by knowing that this force is caused by the floatation of the flap. So, it is necessary to take in consideration the flap's and the fluid's volumetric density.

$$C = g\,h_f\,t_f\,\mathrm{w}_f\cdot\big(\rho\,r_B - \rho_f\,r_G\big)\,, \tag{19}$$

where r_B and r_G are the centre of buoyancy and the centre of gravity of the immersed body, respectively. For the case that is being analysed, it is known, due to the rectangular parallelepiped shape, that the centre of gravity is coincident with the centre of floatation, $r_B = r_G = h_f/2$. So, the hydrostatic restoring moment can be presented in the following way:

$$C = g\,h_f\,t_f\,\mathrm{w}_f\cdot\big(\rho\,\frac{h_f}{2} - \rho_f\,\frac{h_f}{2}\big) = \frac{1}{2}\,g\,t_f\,\mathrm{w}_f\,h_f^2\,\rho\cdot\big(1-\frac{\rho_f}{\rho}\big). \tag{20}$$

The equation of motion of the flap is identical to the equation of a damped harmonic oscillator. So, by using the parameters that were previously defined, the flap's equation of motion can be expressed by:

$$I_f\,\ddot{\theta}(t) + C\,\theta(t) = \mathcal{F} + \mathcal{T}_e(t)\,, \tag{21}$$

where the first function placed on the right side of the *Eq. 21* is called the hydrodynamic torque, $\mathcal{F}$. This function evaluates the pressure differential between the sides of the flap, at $x = -t_f/2$ and $x = +t_f/2$, along its exposed area which results in a force, $F = p\cdot A$. By multiplying this force by an arm it will result in a torque, $T = F\cdot h_f$. So, by using the linearised form of the Bernoulli equation, as presented in Renzi and Dias [20, 21] where $\Delta p = -\frac{\partial(\Delta\phi)}{\partial t}$, the hydrodynamic torque can be defined as:

$$\mathcal{F} = \int_{-h+c}^{-h+h_f+c}\int_{-1/2}^{1/2}\frac{\partial\big(\Delta\Phi^{(R,D)}\big)}{\partial t}\cdot(z+h-c)\,dy\,dz, \tag{22}$$

The diffracted and radiated waves are considered in the equation of motion of the flap by using the velocity potentials defined in *Eq. 16* and in *Eq. 17*. While calculating these velocity potentials it was necessary to use the thin-body approximation assuming that the device's thickness was comparatively smaller than the other dimensions, allowing it to be assumed as being $t_f\approx 0$. With this approximation, the integral calculation of the velocity potential along the flap's surface can be easily obtained, following the method used by Renzi and Dias [20, 21], the *Eq. 22* takes the following format:

$$\mathcal{F} = -\mu\,\ddot{\theta}(t) - \nu\,\dot{\theta}(t) + F\,, \tag{23}$$

where the coefficient that is in phase with the body's acceleration is called added moment of inertia, usually represented by μ, and is given by:

$$\mu = \frac{\pi}{4}\cdot\mathrm{Re}\Big\{\sum_{n=0}^{\infty} f_n\,\alpha_{0n}\Big\}\,. \tag{24}$$

In *Eq. 23*, the coefficient that is in phase with the angular velocity of the flap, $\dot{\theta}(t)$, acts as a damping component which results from the diffracted waves and it is represented by:

$$\nu = \frac{\pi\omega}{4}\,f_0\,\cdot\mathrm{Im}\{\alpha_{00}\}\,. \tag{25}$$

Finally, the excitation torque, F, is given by the following expression:

$$F = \frac{-i\omega\pi}{4}A_I\,f_0\cdot\beta_{00}\,, \tag{26}$$

The resultant equation of motion of the flap which can be obtained by replacing the hydrodynamic torque, $\mathcal{F}$, and its parameters, in *Eq. 21*, will take the following format:

$$\big(I_f + \mu\big) \cdot \ddot{\theta}(t) \; + \; \nu \cdot \dot{\theta}(t) + C \cdot \theta(t) = F + \mathcal{T}_e(t)\,, \qquad (27)$$

The last term in the right side of the *Eq. 27*, $\mathcal{T}_e$, represents the function that defines the torque applied by the generator to the flap and it will be assumed as being a function of time. This function besides being a function of time is usually assumed as being composed by three parts. These can be partly inertial, partly damping and, also, partly elastic. Each of these components is in phase with a single parameter which can be with the acceleration, the velocity or the angular displacement. The resultant function can be expressed by:

$$\mathcal{T}_e(t) = -\mu_{pto}\,\ddot{\theta}(t) - \nu_{pto}\,\dot{\theta}(t) - C_{pto}\,\theta(t)\,, \qquad (28)$$

where μ_{pto}, ν_{pto} and C_{pto} are the inertial, the damping and the elastic properties of the generator, respectively. These parameters are a function of the chosen generator however, they can be optimised to guarantee that the amount of generated power is maximised. As presented by Pizer [19] the power extracted from the motion of a device can be linearly estimated by multiplying the damping force, $F_c = \nu_{pto} \cdot \dot{\theta}(t)$, by the device's angular velocity, $\dot{\theta}(t)$, which results in $P_G = F_c \cdot \dot{\theta}(t)$. This formula can be used when calculating the average generated power over a wave period $T = \frac{2\pi}{\omega}$:

$$P_G = \frac{1}{T} \cdot \int_0^T F_c \cdot \dot{\theta}(t)\, dt = \frac{1}{T} \cdot \int_0^T \big(\nu_{pto} \cdot \dot{\theta}(t)\big) \cdot \dot{\theta}(t)\, dt\,, \qquad (29)$$

To calculate the average generated power, it is necessary to determine the equation of motion of the flap which can be achieved by replacing the generator parameters in the *Eq. 27*. This resultant equation, relates the flap's dimensions with the generator's parameters taking in consideration the diffracted and radiated waves caused by the flap's motion. The resultant equation relates all the forces that are applied on the flap and it is represented by the following equation:

$$\big(I_f + \mu + \mu_{pto}\big) \cdot \ddot{\theta}(t)\, \big(\nu + \nu_{pto}\big) \cdot \dot{\theta}(t) + \big(C + C_{pto}\big) \cdot \theta(t) = F\,, \qquad (30)$$

To obtain the equation that allows the calculation of the motion of the flap it is necessary to calculate the first and second time derivative of θ. By effectuating the derivatives, the equation will result in the following expression:

$$\theta(t) = \frac{F}{-\omega^2 \cdot \big(I_f + \mu + \mu_{pto}\big) - i\,\omega \cdot \big(\nu + \nu_{pto}\big) + \big(C + C_{pto}\big)} \qquad (31)$$

With this equation it is possible to determine the flap's amplitude of oscillation when it is forced to oscillate by the incident waves with a constant frequency, ω. The presence of the generator influences the amplitude of response of the flap and, as can be concluded by analysing *Eq. 29*, the average generated power is linearly proportional to the damping coefficient of the generator and to the flap's rotational velocity. It is possible to replace *Eq. 31* in the formula that defines the average generated power, shown in *Eq. 29*. This substitution results in the following equation:

$$P_G = \frac{1}{2} \cdot \frac{\omega^2 \cdot \nu_{pto} \cdot \big|F\big|^2}{\big[-\omega^2 \cdot (I + \mu + \mu_{pto}) + C + C_{pto}\big]^2} \cdot \frac{\nu_{pto} \cdot \big|F\big|^2}{\big(\nu + \nu_{pto}\big)^2}\,, \qquad (32)$$

The flap's rotational velocity is dependent of the generator's damping coefficient and the generated power is dependent of both of these parameters. To maximise the generated power, it is necessary to determine the value of the optimum damping coefficient, which can be accomplished by derivating *Eq. 29* in order to ν_{pto}:

$$\frac{\partial P_G}{\partial \nu_{pto}} = 0\,, \qquad (33)$$

It results in the following equation:

$$\nu_{pto} = \nu_{opt} = \sqrt{\frac{\big(-\omega^2 \cdot (I + \mu + \mu_{pto}) + C + C_{pto}\big)^2}{\omega^2}} + \nu \qquad (34)$$

Even though the optimum value for the generator's damping as been determined, it is necessary to determine the device's natural frequency. It can be calculated using the following equation:

$$\omega_n = \sqrt{\frac{k_{eq}}{M_{eq}}} = \sqrt{\frac{C + C_{pto}}{I + \mu + \mu_{pto}}}\,, \qquad (35)$$

The oscillations made by a body, when it is being excited by an external force, are defined as having the same frequency as the excitation force. The devices' amplitude of oscillations is a function of the waves' frequency and as close as they get to the natural frequency of the device, the amplitude of the oscillations will increase, as can be concluded by replacing *Eq. 35* in *Eq. 31*. After some algebraic operations, the substitutions give the following equation:

$$\theta(t) = \frac{F}{\omega_n^2 \cdot \big(I_f + \mu + \mu_{pto}\big) \left(1 - \big(\frac{\omega}{\omega_n}\big)^2\right) - i\,\omega \cdot \big(\nu + \nu_{pto}\big)} \qquad (36)$$

The equations that were shown in this chapter enable the possibility of analysing several configurations for an oscillating surge wave energy converter. For example, it can be a completely immersed or a surface piercing device while varying the remaining device's dimensions. The flap's dimensions can be changed allowing the possibility of evaluating the effects of these changes in the evaluated outputs. There are several possible configurations that can be analysed by changing each of these parameters:

- Flap width;
- Flap height;
- Flap thickness;
- Support height;
- Local water depth;
- Wave period/frequency;

4. Results

The goal was to analyse both possibilities for the *OSWECs* which can be completely submerged or with their upper surface extending above the water's free surface. Yet, solely the results obtained for the surface piercing devices have been validated experimentally by other authors. So, the theoretically obtained results for these surface piercing devices will be compared with the results obtained by van't Hoff [28] and afterward published in an article by Renzi and Dias [20]. These enabled the possibility of determining how closely the theoretical results fit with other scientific publications.

For the validation of the theoretical results, experiments have been realised to enable the possibility of concluding if the semi-analytical equations can be used for the evaluation of both surface piercing and submerged *OSWECs*.

4.1. Semi-analytical analysis of the WEC parameters

The first steps for the formulation of an analysis is the definition of the parameters that will be evaluated which can be characterised as being input parameters and output values. The former, the output values, are the ones by which a device is usually analysed and that enable the possibility of concluding about the viability for further investigation or even for

the device to be deployed in open waters. The output values that were analysed are the following:

- Added Inertia;
- Radiation and Optimum Generator Damping;
- Response Angle;
- Excitation Torque;
- Average Generated Power;
- Capture Factor;

Solely one of these values had a restriction to its value, similarly to what Henry [13], Tom et al. [27], Whittaker and Folley [31] did during their analyses. The device's amplitude of oscillation needs to be limited to a certain value due to the generator's range of motion. However, the value for the maximum amplitude of oscillation isn't consensual among the published articles. There are some authors who have decided to use maximum values for the pitch oscillations of 30°, such as Tom et al. [27] and Whittaker and Folley [31], while Henry [13] used the values of 40° and Chehaze et al. [6] of 50°. While, in extreme seas the article of Wei et al. [29] established that the oscillations could go as high as 75°. These values are too widely spread to be able to conclude about which one should be chosen. So, by taking a conservative approach, only the values of the articles that have realised model experiments were considered, which are the ones of Henry [13] and Chehaze et al. [6]. So, the condition that has been imposed is:

1. The device's amplitude of pitch oscillations cannot surpass $\theta_{max} = 40$ [°];

By imposing this limitation, the results obtained with the semi-analytical equations led to conclude that an increase to the flap's width will result in an increase to the generated power, having a similar effect to the capture factor and to the natural period. Comparing the results obtained for the variation of the main device's parameters, the flap's width is the most effective in increasing the generated power while causing a smaller variation to the device's natural period, enabling it to still have its natural period on the same bandwidth as the incident waves' periods.

While evaluating the effects caused by the variation of the flap's height, it is necessary to separate the results for the devices that are surface piercing and the ones that are completely submerged. This is because the results for these devices led to different conclusions so, they need to be evaluated separately. While the increase of the flap's height for the submerged device is parabolic, reaching the maximum generated power for smaller heights than the ones for surface piercing devices with zero freeboard, the results for the surface piercing devices led to other conclusions. So, the results for the submerged devices led to conclude that is more viable to deploy a submerged device with negative freeboard than a device with zero freeboard while for the surface piercing devices the increase of the flap's height causes an increase to the average generated power, reaching similar values to the ones obtained with the submerged devices. Such conclusion wasn't expected and the experimental tests might help settling if these equations may be used, as they are, for submerged devices.

Another dimension that was evaluated, even though it was hindered to be correctly evaluated, was the flap's thickness. The thickness wasn't considered while integrating the velocity potentials around the device's flap however, it was considered while calculating the flap's inertia and the hydrostatic restoring moment. The results led to conclude that the increase in flap's thickness will result in higher values of generated power, increasing the capture factor and decreasing the device's natural period, with similar conclusions being withdrawn by Henry [13].

The remaining parameter that was evaluated is the device's support height. This parameter, since it cannot extract energy from the incident waves, it should be minimised enabling an increase of the flap's height [13]. So, the values for which the support height was evaluated varied between a small range of *1 m* up to *2 m* and it almost did not effect the generated power, the capture factor or the natural period. The small change however, caused a slight increase in generated power and in capture factor but it was relatively much smaller than the changes caused by the flap's height variation.

The results obtained with semi-analytical equations caused by the variation of the device's dimensions can be checked in *Table 2*.

Table 2: Effects caused by the increase of the device's dimensions

Device's dimension	**Generated Power**	**Capture Factor**	**Natural Period**
Flap's Width	↗	↗	↗
Flap's Height (submerged)	↗	↗	↗
Flap's Height (surface piercing)	↗	↗	↗
Flap's Thickness	↗	↗	↘
Support Height	≈ 0	≈ 0	≈ 0

4.2. Experimental Tests

The experiments took place in the facilities of the Portuguese National Laboratory of Civil Engineering were they have several wave tanks and three wave flumes. The experiments were realised in one of their flumes which has a total length of *38.0 m* and the wave maker occupies the initial *5.43 m*.

In smaller wave flumes, like the one where these experiments were realised, it is usual that one of the side walls converges to the centre of the flume until reaching a smaller width. However, this flume has been characterised by having a peculiar geometry [7] because both of its side walls converge from *1.0 m* up to *0.60 m* of width. The analysed model devices were placed in the testing area where the width was of *0.60 m* and the bottom was sloped with a gradient of *1:136*, as shown in *Figure 2*.

Three different models were analysed, with two of them having surface piercing dimensions and one of them being completely submerged. These were analysed at different scales with a completely submerged and a surface device at a scale of *1:90* and a surface piercing device at a scale of *1:45*. The scales for which the devices were analysed were limited by the dimensions of the wave flume and also by the real scale dimensions that were being analysed.

During the experiments, four variables where measured which were: the flap's oscillation angle, the excitation torque applied on the flap and the waves' amplitude and period. For the measurement of the flap's oscillation angles, two potentiometers were coupled to the flap's axis of rotation which enabled the measurements of both the amplitude and flap's location rate of change, i.e., its velocity. For the measurement of the excitation torque, two load cells were placed in contact

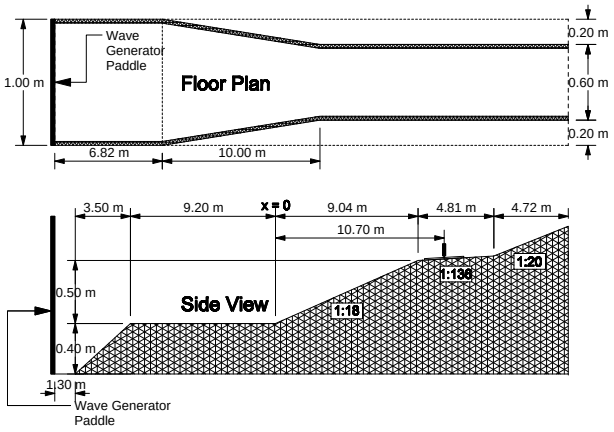

Figure 2: Model of the wave flume with the location of the *OSWEC*

with the up and downstream surfaces of the flap. Finally, for the measurement of the waves' amplitude and period, wave probes were placed at both the upstream and downstream location of the device.

The device's response to the incoming waves was analysed and the incident waves were based on characteristics determined by Rusu and Guedes Soares [23] for the Portuguese shore. In real scale, the waves' periods range between *4-14s* and the waves' amplitude was assumed as being unitary.

4.2.1. Device at 90th scale

The device's dimensions were based on the results obtained with the semi-analytical equations and also by analysing the dimensions of the devices that are being studied in open waters. For this scale, it was also considered the article authored by Renzi and Dias [21] where they evaluated the influence caused by the flume's side walls on the device's results. When the ratio between the device's width and the flume's width is larger than *0.4* the proximity to the side walls will start to influence the results by varying the excitation forces applied on the flap. So, the devices at this scale had a width of *0.2 m*, resulting in a ratio of 1/3. The dimensions of the flaps that were analysed can be checked on *Table 3*.

Table 3: Comparison between real scale and experimental values for the *90* th model scale

Scale	**1:1**		**1:90**	
Type	**Sub.**	**Surf. Pier.**	**Sub.**	**Surf. Pier.**
Flap's Width [m]	18.00	18.00	0.20	0.20
Flap's Height [m]	7.20	9.90	0.08	0.11
Flap's Thickness [m]	1.80	1.80	0.02	0.02
Support Height [m]	3.60	3.60	0.04	0.04
Wave amplitude [m]	0.90	0.90	0.01	0.01
Depth [m]	12.00	12.00	0.133	0.133

Due to the limitations of the wave maker, it wasn't possible to evaluate the two lowest wave periods, which were the ones equivalent to *4* and *5 s* periods. However, by scaling the remaining real waves' periods and amplitude to the model scale, the values that were used to excite the device are shown in *Table 4*.

Table 4: Comparison between the pretended and the obtained values for the periods and the amplitudes of the waves in a depth of *13.3 cm*

Voltage *[V]*	**P$_{PRE}$** *[s]*	**P$_{OBT}$** *[s]*	**A$_{PRE}$** *[m]*	**A$_{OBT}$** *[m]*
0.23	0.630	0.630	0.010	0.010
0.207	0.740	0.740	0.010	0.010
0.21	0.840	0.840	0.010	0.010
0.21	0.950	0.950	0.010	0.011
0.205	1.050	1.050	0.010	0.010
0.215	1.160	1.160	0.010	0.010
0.225	1.260	1.260	0.010	0.010
0.26	1.370	1.370	0.010	0.010
0.205	1.480	1.480	0.010	0.008

4.2.1.1 Submerged device

The first experiment was with the submerged device and, as stated previously, the semi-analytical equations were modified to allow the analysis of this type of devices. So, the experimental tests will either validate the theoretical results or enable to conclude that the equations need to be modified when evaluating submerged devices. The results obtained experimentally and the theoretical results for the submerged device can be checked in *3(a)* and in *3(b)*.

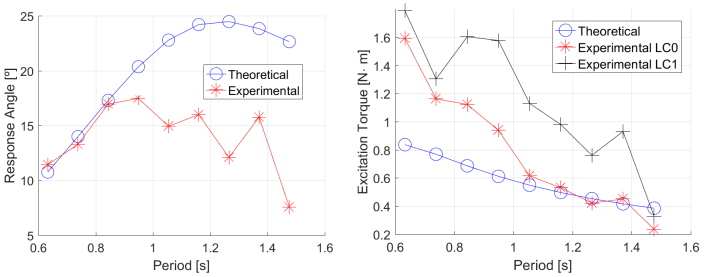

(a) Comparison of values obtained for the response angle

(b) Comparison of values obtained for the excitation force

Figure 3: Comparison between the experimental and theoretical results for the submerged device at a scale of *1: 90*

Even though for small wave periods the results for the response angle fit surprisingly well, for larger wave periods the results start to diverge from each other. So, for the calculation of the flap's response angle, the equations need to be corrected to take into account this divergence for the larger wave periods.

The forces applied on the flap were measured with two load cells where one was placed on the upstream surface of the device, represented by *LC0*, and the other on the downstream surface, represented by *LC1*. The results shown in *3(b)* allow to conclude that the experimental results follow the same tendency as the theoretical values, reaching similar values for the larger wave periods.

4.2.1.2 Surface piercing device

The support of the flap did not change between the experiments for the devices with the same scale, solely the dimension of the flaps changed. Comparatively, this flap had more *3 cm* than the submerged flap which enabled it to have a

positive freeboard of *1.7 cm*. This small change led to a significant increase of the excitation torque for smaller wave periods while keeping the same tendency as the theoretical results. Even though the response angle results obtained for the submerged device fit better the theoretical results for the smaller wave periods, for this flap height it comparatively fits better the periods bandwidth.

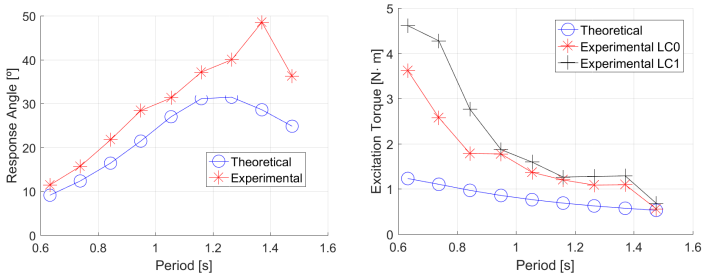

(a) Comparison of values obtained for the response angle (b) Comparison of values obtained for the excitation force

Figure 4: Comparison between the experimental and theoretical results for the surface piercing device at a scale of *1: 90*

The theoretical results solely consider the linear terms and, as Evans [11] stated, these represent a prediction of the values that will be obtained in open waters.

Analysing the results shown in *Figure 4*, it is possible to state that the results obtained for the surface piercing device show a better correlation with the theoretical results than the results obtained with the submerged device.

4.2.2. Device at 45^{th} scale

The main reason for analysing the devices at 90^{th} was due to the results presented by Renzi and Dias [21]. He concluded that to minimise the influence caused by the side walls on the results, the ratio between the flap's width and the flume's width should not be larger than *2/5* yet, besides the 45^{th} scale model, a larger device was studied with a width ratio of *2/3*, resulting in a 45^{th} scale model, as shown in *Table 5*.

Table 5: Comparison between real scale and experimental values for the *45* th model scale

Scale	**1:1**	**1:45**
Type	**Surf. Pier.**	**Surf. Pier.**
Flap's Width [m]	18.00	0.40
Flap's Height [m]	9.90	0.22
Flap's Thickness [m]	1.80	0.04
Support Height [m]	3.60	0.08
Wave amplitude [m]	0.90	0.02
Depth [m]	12.00	0.266

4.2.2.1 Surface piercing device

To evaluate the device's response to the same incident waves' periods, it was necessary to scale the periods given by Rusu and Guedes Soares [23] for the Portuguese waves that ranged between *4-14s*. However, similarly to what happened while evaluating the 90^{th} model scale periods, the wave maker was limited and could not evaluate the two lowest wave periods. So, the resultant scaled wave periods range between *0.894 s* up to *2.087 s* with a time step between each period of *0.149 s*, as shown in *Table 6*.

Similarly to the procedure used for the smaller model scale, these experiments also used two potentiometers for the measurements of the flap's oscillations, two load cells for the measurement of the excitation torque and one wave probe for the measurement of the waves' amplitudes and periods in *6* different locations, where *3* of which were placed upstream of the device and the other *3* at a location downstream from the device's position.

Table 6: Comparison between the pretended and the obtained values for the periods and the amplitudes of the waves in a depth of *26.6 cm*

Voltage *[V]*	**PPRE** *[s]*	**POBT** *[s]*	**APRE** *[m]*	**AOBT** *[m]*
0.46	0.894	0..89	0.020	0.020
0.43	1.043	1.040	0.020	0.019
0.48	1.192	1.190	0.020	0.021
0.44	1.341	1.340	0.020	0.021
0.52	1.490	1.490	0.020	0.021
0.59	1.640	1.640	0.020	0.024
0.48	1.789	1.790	0.020	0.014
0.69	1.938	1.940	0.020	0.023
0.56	2.087	2.090	0.020	0.015

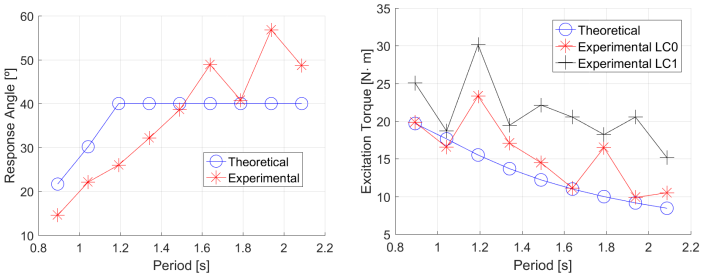

(a) Comparison of values obtained for the response angle (b) Comparison of values obtained for the excitation force

Figure 5: Comparison between the experimental and theoretical results for the surface piercing device at a scale of *1: 45*

The results shown in *5(a)*, can be compared to the ones obtained for the smaller scale device of the same type. However, it is clear that the theoretical values are restrained by the upper limit to the flap's oscillation angle so, the amplitude can no longer reach values as the ones obtained experimentally. Yet, for the smaller periods, the values are comparable and follow the same tendency as the theoretical results.

The results for the excitation torque represented in *5(b)*, show that the experimental values followed the same tendency as the theoretical values and for some wave periods they obtained almost equal results.

It was expected that the influence caused by the side walls would have a larger impact in the measured results yet, the experimental results still followed closely the theoretically obtained values similarly to the ones for the smaller scale surface piercing device.

5. Conclusions

This work analysed the hydrodynamics of an oscillating surge wave energy converter and evaluated the possibility of using the semi-analytical equations for analysing both type of devices, the submerged type and surface piercing type.

The obtained theoretical results led to conclude that the increase of the flap's width would result in a higher excitation torque leading to the chance of increase the generator's damping which would result in a higher generated power. Yet,

the increase of the flap's width will obligate the need of considering the device's directionality in relation to the waves' direction of propagation. Even though, it has been established theoretically that the increase of the flap's width will enable the chance of generating more power, that variable could not be individually experimentally tested.

The increase of the flap's height can also be used to increase the generated power [13]. This is accomplished by having a device whose flap covers the whole water column leading to a lower amount of wave energy surpassing the device's flap. An increase to the flap's height resulted in an increase of the generated power however, it had a smaller significance than when comparing with the results for the variation of flap's width. Either way, these two dimensions should be both increased, as proposed by Henry [13].

The remaining dimension that defines the device's flap is its thickness. Yet, due to the assumptions that have been settled for the semi-analytical equations, they are hindered to correctly calculate the effects caused by the variation of the flap's thickness. While developing the equations, the thin-body approximation has been assumed easing the calculation of the velocity potential. By doing so, the velocity potential is equal between both upstream and downstream surfaces of the flap thus not considering the flap's thickness. Even though there's this slight problem, and as was proposed by Henry [13], the increase of the flap's thickness could be used to change the device's natural period mainly due to the increase of its thickness which would result in an increase of the flap's added inertia leading to a decrease of the natural period, assuming that the variation would be smaller for the remaining parameters.

There was one last dimension that was analysed which was the support height. This was one of the parameters that registered very small changes when varying its value. However, the variation of this parameter could be realised in accordance with the increase of the flap's height, enabling the possibility of keeping a constant value for the freeboard. Actually, this idea of decreasing the support height while increasing the flap's height was proposed by Henry [13] and it enabled the possibility of increasing the area that is going to absorb the incident waves' energy.

These conclusions should have been confirmed experimentally however, solely a few experiments could be realised. So, and since that the flap's height is one of the main characteristics that distinguishes this type of devices, the variation of the flap's height was the parameter that was evaluated experimentally. The experimental results led to conclude that the theoretical equations, for the surface piercing cases, followed the correct tendency with the variation of the waves' period. Yet, the experimental results obtained for the submerged device led to conclude that these equations should be revised in order to take into account the energy that passes over the device's submerged flap.

References

[AWE] AW Energy. `http://aw-energy.com/pt-pt`. (Accessed on 25/01/2017).

[GTE] Gte16_aquamarine_power_newsletter.pdf. `http://londonresearchinternational.com/wp-content/uploads/2014/06/GTE16_Aquamarine_Power_Newsletter.pdf`. (Accessed on 11/19/2017).

[3] Burman, K. (2009). *Ocean Energy Technology Overview*. Number July.

[4] Cameron, L., Doherty, R., Henry, A., Doherty, K., Hoff, J. V., Kaye, D., Naylor, D., Bourdier, S., and Whittaker, T. (2010). Design of the Next Generation of the Oyster Wave Energy Converter. *3rd International Conference on Ocean Energy*, pages 1–12.

[5] Charlier, R. H. and Justus, J. R. (1993). *Ocean energies : environmental, economic, and technological aspects of alternative power sources / Roger H. Charlier and John R. Justus*. New York : Elsevier Amsterdam.

[6] Chehaze, W., Chamoun, D., Bou-Mosleh, C., and Rahme, P. (2016). Wave Roller Device for Power Generation. *Procedia Engineering*, 145:144–150.

[7] Conde, J. M. P., Capitão, R., and Fortes, M. G. N. C. J. (2012). Comparação de técnicas de absorção passiva de ondas com avaliação da agitação incidente e refletida em canal. (2):131–134.

[8] Dhanak, M. R. and Xiros, N. I. (2016). *Handbook of Ocean Engineering*.

[9] European Marine Energy Centre (2009). *Tank Testing of Wave Energy Conversion Systems*.

[10] Evans, D. V. (1976). A theory for wave-power absorption by oscillating bodies. *Journal of Fluid Mechanics*, 77(01):1–25.

[11] Evans, D. V. (1986). The Hydrodynamic Efficiency of Wave-Energy Devices. In Evans, D. V. and Falco, A. F. O., editors, *Hydrodynamics of Ocean Wave-Energy Utilization: IUTAM Symposium Lisbon/Portugal 1985*, chapter 1, pages 1–34. Springer-Verlag Berlin Heidelberg, Lisbon.

[12] Gunn, K. and Stock-Williams, C. (2012). Quantifying the global wave power resource. *Renewable Energy*, 44:296–304.

[13] Henry, A. (2008). *The hydrodynamics of small seabed mounted bottom hinged wave energy converters in shallow water*. PhD thesis, The Queen's University of Belfast.

[14] Inman, D. L. and Brush, B. M. (1973). The Coastal Challenge. *Science*, pages 20–32.

[15] Kinsman, B. (1965). *Wind waves: their generation and propagation on the ocean surface / Blair Kinsman*. Prentice-Hall Englewood Cliffs, N.J.

[16] Leishman, J. M. and Scobie, G. (1976). The development of wave power - A Tecnho-Economic Study. Technical report, National Engineering Laboratory, Glasgow.

[17] Newman, J. N. (1962). The Exciting Forces on Fixed Bodies in Waves. *Journal of Ship Research, Society of Naval Architects and Marine Engineers*, 6:1–10.

[18] Newman, J. N. (1975). Interaction of waves with two-dimensional obstacles: a relation between the radiation and scattering problems. *Journal of Fluid Mechanics*, 71(2):273–282.

[19] Pizer, D. (1994). *Numerical Modelling of Wave Energy Absorbers*. Number V.

[20] Renzi, E. and Dias, F. (2012). Resonant behaviour of an oscillating wave energy converter in a channel. *Journal of Fluid Mechanics*, 701(2007):482–510.

[21] Renzi, E. and Dias, F. (2013). Hydrodynamics of the oscillating wave surge converter in the open ocean. *European Journal of Mechanics, B/Fluids*, 41:1–10.

[22] Ross, D. (1979). *Energy from the waves: the first-ever book on a revolution in technology / by David Ross*. Pergamon Press Oxford ; New York.

[23] Rusu, E. and Guedes Soares, C. (2009). Numerical modelling to estimate the spatial distribution of the wave energy in the Portuguese nearshore. *Renewable Energy*, 34(6):1501–1516.

[24] Salter, S. H. (1974). Wave power. *Nature*, 249(June 1974):720.

[25] Silva, D., Bento, A. R., Martinho, P., and Guedes Soares, C. (2015). High resolution local wave energy modelling in the Iberian Peninsula. *Energy*, 91:1099–1112.

[26] Srokosz, M. a. and Evans, D. V. (1976). A theory for wave-power absorption by two independently oscillating bodies. *Journal of Fluid Mechanics*, 90(02):1–25.

[27] Tom, N., Wright, A., Lawson, M., and Yu, Y.-h. (2015). Preliminary Analysis of an Oscillating Surge Wave Energy Converter with Controlled Geometry. *European Wave and Tidal Energy Conference*, (September):1–10.

[28] van't Hoff, J. (2009). *Hydrodynamic modelling of the oscillating wave surge converter*. PhD thesis, Queens University Belfast.

[29] Wei, Y., Rafiee, A., Henry, A., and Dias, F. (2015). Wave interaction with an oscillating wave surge converter, Part I: Viscous effects. *Ocean Engineering*, 104:185–203.

[30] Whittaker, T. and Folley, M. (2009). Analysis of the nearshore wave energy resource. *Renewable Energy*, 34(7):1709–1715.

[31] Whittaker, T. and Folley, M. (2012). Nearshore oscillating wave surge converters and the development of Oyster. *Philosophical transactions. Series A, Mathematical, physical, and engineering sciences*, 370(1959):345–64.